Korean J. Chem. Eng., **19**(5), 791-796 (2002)

The Effects of Oxygen Flow Rate and Anion Doping on the Performance of the $LiNiO_2$ Electrode for Lithium Secondary Batteries

Sang Ho Park*, Ki Soo Park, Myung Hun Cho, Yang Kook Sun*, Kee Suk Nahm†, Yun Sung Lee and Masaki Yoshio****

School of Chemical Engineering and Technology, College of Engineering,
Chonbuk National University, Chonju 561-756, Korea
*Department of Industrial Chemistry, College of Engineering, Hanyang University, Seoul 133-791, Korea
**Department of Applied Chemistry, Saga University, 1 Honjo, Saga 840-8502, Japan
(*Received 19 April 2002 • accepted 11 July 2002*)

Abstract−This work presents the effects of O_2 flow rate and S-doping on structural and electrochemical properties of $LiNiO_2$. Layered $LiNiO_2$ were prepared using a sol-gel method. It was found that oxygen plays an important role in the crystallization of layered $LiNiO_2$. The deficiency of oxygen in the crystallization process induced the inclusions of impurities and cubic rock-salt structure in $LiNiO_2$ powders. For $LiNiO_2$ prepared at high O_2 flow rates, the electrode delivered high initial discharge capacity with a relatively good retention rate. S-doped $LiNiO_2$ not only stabilized the structural integrity of the electrode material, but also increased the electrode performance.

Key words: Li Battery, $LiNiO_2$, Oxygen Effect, Anion Doping, Structural and Electrochemical Characterizations

INTRODUCTION

$LiNiO_2$ is a promising cathode material for the lithium secondary battery due to its natural abundance and non-toxicity [Delmas, 1989; Reimers et al., 1993]. In spite of the advantages, $LiNiO_2$ has not been widely used as a cathode material for lithium secondary batteries because it is difficult to synthesize stoichiometric $LiNiO_2$ [Dahn et al., 1990].

Many research groups have employed a variety of synthetic conditions in order to overcome this barrier, and they have reported how the synthetic parameters influence the structural and electrochemical properties of synthesized materials. Among the parameters, some groups have found that kind and flow rate of atmospheric gas during calcination have a serious impact on the crystallization of the synthesized $LiNiO_2$ which significantly influences the electrode performance. Ohzuku [Ohzuku et al., 1993] and Wang [Wang et al., 1998] measured charge-discharge properties of $LiNiO_2$ powders synthesized at 750 °C under the flow of oxygen or air, and reported that the discharge capacity of $LiNiO_2$ synthesized in O_2 was much higher than that in air, and that capacity fading rapidly occurred in air, whereas it was significantly prevented in an O_2 atmosphere. Meanwhile, many researchers have reported that the crystal structure of $LiNiO_2$ can be stabilized by substituting cation or anion of $LiNiO_2$ with other corresponding ions. Partial substitution of Ni for $LiNiO_2$ with some transition metals such as Al, Co, Ga, Mg, Ti, etc., has been widely studied to improve the cycle life of the electrode [Ohzuku et al., 1997; Nitta et al., 1995; Banov et al., 1995; Nishida et al., 1997; Arai et al., 1997; Gao et al., 1998; Kubo et al., 1997; Lee et al., 1999]. The stabilization of $LiNiO_2$ has also been attempted by substituting O for $LiNiO_2$ with fluorine, resulting in the significant improvement of $LiNiO_2$ cycleability during the intercalation/deintercalation of lithium ions [Morales et al., 1990]. We also found that anion doping with sulfur was very effective in stabilizing the crystal structure of $LiMn_2O_4$ [Choi et al., 1995].

In this work, we have synthesized $LiNiO_2$ as a function of the oxygen flow rate (100-900 sccm) using the sol-gel method. S-doping of $LiNiO_2$ was attempted to improve the stability of the $LiNiO_2$ crystal structure. For the first time, we have synthesized S-doped $LiNiO_{2-y}S_y$ powders. The structural and electrochemical properties of the synthesized materials were investigated by using various analytic techniques. Gas composition was measured during the calcination of $LiNiO_2$ precursors.

EXPERIMENTAL

$LiNiO_2$ powders were synthesized by a sol-gel method. Stoichiometric amounts of Li [$Li(CH_3COO)\cdot 2H_2O$] and Ni acetate [$Ni(CH_3COO)_2\cdot 4H_2O$] salts (cationic ratio of Li : Ni=1 : 1) were dissolved in DI water. This prepared solution was introduced drop by drop into continuously agitated aqueous adipic acid solution, which was used as a chelating agent. The molar ratio of adipic acid to total metal ions was fixed to unity. The mixed solution was evaporated at 70-80 °C to make a transparent sol. The sol was turned into a viscous transparent gel by further evaporation. The gel precursors were decomposed at 450 °C for 10 h in a box furnace to eliminate organic components. The decomposed powders were post-calcined at 750 °C under oxygen flow for 14 hrs in a quartz tubular reactor as a function of oxygen flow rate (100-900 sccm), and the heating and cooling rate of the powders was 1 °C/min to prevent cation mixing in $LiNiO_2$. For the preparation of S-doped $LiNiO_2$, the precalcined powders were mixed with a stoichiometric amount of sulfur powders and were sufficiently grounded. These mixed powders were post-calcined at 750 °C in a flow of oxygen for 14 hrs. The cooling rate of the powders maintained 1 °C/min to prevent cation mixing in $LiNiO_2$.

†To whom correspondence should be addressed.
E-mail: nahmks@moak.chonbuk.ac.kr

After the synthesis, amounts of Li, Ni, and S in the synthesized materials were analyzed with an inductively coupled plasma (ICP, Himadachi) and sulfur analyzer (LECO Co., CS 444), respectively, to determine their actual chemical composition. The oxygen content was determined via mass balance. The structural properties of the synthesized powders were investigated by using powder X-ray diffraction (XRD, D/Max-3A, Rigaku) with a Cu-Kα target. Rietveld refinement was carried out by using XRD data to obtain lattice parameters of synthesized powders.

A quadrapole mass spectroscopy (QMS, HAL2/511, Hiden) was employed to analyze gas composition evolved during the calcination of as-prepared gel precursors (0.5 g) under a flow of 250 ml/min O_2. The temperature of the sample was monitored just below the sample holder and raised with a heating rate of 5 °C/min with a PID (proportional-integral-derivative) controller. The outlet of the reactor was connected to the QMS by a quartz capillary tube (0.5 mm).

The electrochemical characterization was performed using CR2032 coin-type cells. For assembling the electrochemical test cell, the cathode was fabricated with a carefully weighed active material (20 mg) and a conductive binder (13 mg). This was pressed upon a 25 mm^2 stainless steel mesh used as the current collector at 300 kg/cm^2 and dried at 200 °C for 5 hours in an oven. This cell consisted of a cathode and a lithium metal anode (Cyprus Foote Mineral Co.) separated by a porous polypropylene film as the separator (Celgard 3401). The electrolyte was a 1 M $LiPF_6$-ethylene carbonate (EC)/dimethyl carbonate (DMC) (1 : 2 by volume). The cell was assembled in an argon-filled dry box and was tested at room temperature. The cell was charged and discharged at a current density of 0.4 mA/cm^2 (C/3) with cut-off voltages of 3.0 to 4.3 V (vs. Li/Li^+).

RESULTS AND DISCUSSION

1. Gas Analysis During Decomposition of Gel Precursor

In order to investigate how the O_2 flow rate influenced the synthesis of crystallized $LiNiO_2$, the composition of the gas mixture produced during the decomposition of the $LiNiO_2$ gel precursor was analyzed by using QMS. The QMS was operated at 10^{-5} torr at room temperature during the analysis. The synthesized precursor (0.5 g) was loaded on a sample holder in a tubular quartz reactor, heated by a tubular furnace. The temperature was monitored just below the sample holder and raised with a heating rate of 5 °C/min with a PID controller. The outlet of the reactor was connected to the QMS by using a quartz capillary tube (0.5 mm). In the connection, a two-stage-precision-needle-valve was used to overcome the pressure difference between the reactor and the QMS system. During analysis, the reactor was evacuated with a vacuum pump and oxygen was directed through the reactor at 250 cm^3/min.

Fig. 1 shows the partial pressures of gaseous species that evolved during the decomposition of the gel precursor as a function of the temperature. It is observed that the moisture in the precursor begins to desorb at above 100 °C. It seems that most of the starting materials used for the synthesis begin to decompose at about 400 °C, which is well consistent with TGA and DTA analyses observed in our previous report [Lee et al., 1999]. The partial pressures of CO_2, H_2O, and H_2 gases greatly increase at around 400 °C, whereas the partial pressure of CO is much smaller than that of CO_2. These

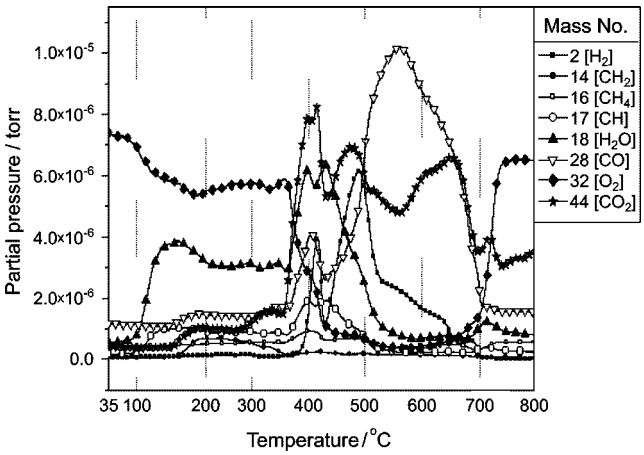

Fig. 1. Plots of partial pressures of gaseous species evolved from $LiNiO_2$ gel precursor during calcination as a function of decomposition temperature.

evolved gases mainly originate from the decomposition of starting materials and chelating agent. It is very interesting to see that the partial pressure of oxygen rapidly decreases from about 400 °C and remains at a very low level in the temperature range from 400-700 °C. At above 700 °C, the partial pressure of oxygen recovers its original value and levels off as the temperature further increases. This indicates that most of the crystallization of $LiNiO_2$ occurs in the temperature range of 400-700 °C and the synthetic reaction is terminated at about 700 °C.

The starting materials began to decompose at about 400 °C to produce a gas mixture that mainly consisted of CO_2 and H_2O. It is natural to see the production of CO_2 and H_2O from the starting materials in the presence of O_2 during the decomposition process. Meanwhile, it seems that the primary evolution of CO and CO_2 in the crys-

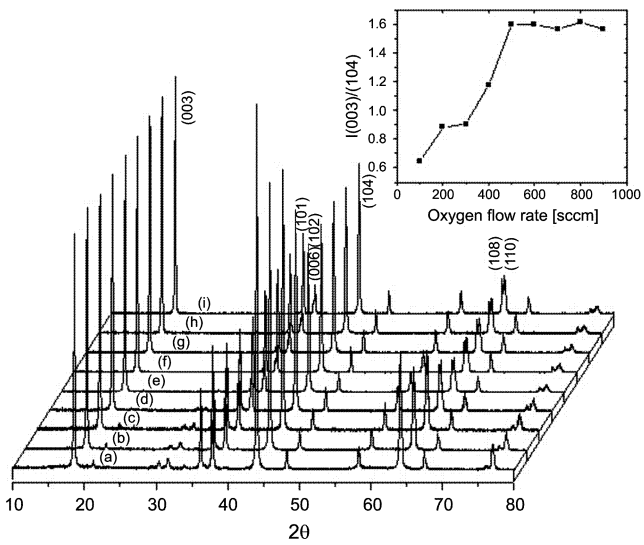

Fig. 2. X-ray diffraction patterns of $LiNiO_2$ at various oxygen flow rates, (a) 100 sccm, (b) 200 sccm, (c) 300 sccm, (d) 400 sccm, (e) 500 sccm, (f) 600 sccm, (g) 700 sccm, (h) 800 sccm, and (i) 900 sccm. The powders were prepared by using a sol-gel method at a pre-calcination temperature of 450 °C in air and calcined again at 750 °C in O_2.

tallization process is due to the oxidation of deposited carbonaceous residues in the presence of oxygen. The above observation clearly demonstrates that oxygen plays an important role for the synthesis of highly crystallized $LiNiO_2$, as suggested in previous experiments [Ohzuku et al., 1993; Wang et al., 1998].

2. Effect of Oxygen Flow Rate

Fig. 2 shows typical XRD spectra for $LiNiO_2$ powders prepared at 750 °C for 14 hrs as a function of oxygen flow rate (100-900 sccm). XRD spectra show that all the synthesized samples have a typical $LiNiO_2$ layered structure with a space group $R\bar{3}m$. Any impurity-related peaks are not observed from the XRD spectrums for $LiNiO_2$ powders synthesized at O_2 flow rates of 500-900 sccm, but the powders prepared at O_2 flow rates of 100-400 sccm exhibit XRD peaks of LiOH, Li_2CO_3, and Li_2O impurities at 2θ=22, 30, and 33°, respectively. The XRD peak intensities of LiOH, Li_2CO_3, and Li_2O impurities decrease as the O_2 flow rate is increased from 100 to 400 sccm. At lower oxygen flow rates, it is considered that carbonaceous residues, originating in starting materials during the pre-calcinating process, are not completely removed from the samples and react with lithium to form various impurities during the post calcinating process. All the peaks that appeared on the XRD patterns were identified with the characteristic peaks of $LiNiO_2$ reported in the X-ray powder data file of JCPDS as well as previously reported works [Ohzuku et al., 1993].

Shown in the upper inset in Fig. 2 is the intensity ratio of (003) and (104) peaks obtained from the XRD spectra of Fig. 2 as a function of the O_2 flow rate. As the O_2 flow rate increases, the intensity ratio of (003) and (014) peaks increases up to 500 sccm and remains at an almost constant value above 500 sccm. According to Morales et al. [Morales et al., 1990], an investigation of the structure of $LiNiO_2$ powders by using the XRD shows that the (003) peak occurs from the diffraction of the layered rock-salt structure ($R\bar{3}m$), whereas the (104) peak appears from both the diffractions of layered and cubic rock-salt structures. In addition, Fig. 1 shows that the splitting of (101) and (006) peaks and (108) and (110) peaks increase with an increase in the O_2 flow rate up to 500 sccm and becomes apparent above 500 sccm. The increase of the splitting of the peaks provides strong evidence for the formation of the $R\bar{3}m$ layered rock-salt phase, which has a stable structure and a high electrical conductivity [Choi et al., 1995]. Summarizing the above structural analysis, the best-crystallized $LiNiO_2$ powders are synthesized at O_2 flow rates above 500 sccm.

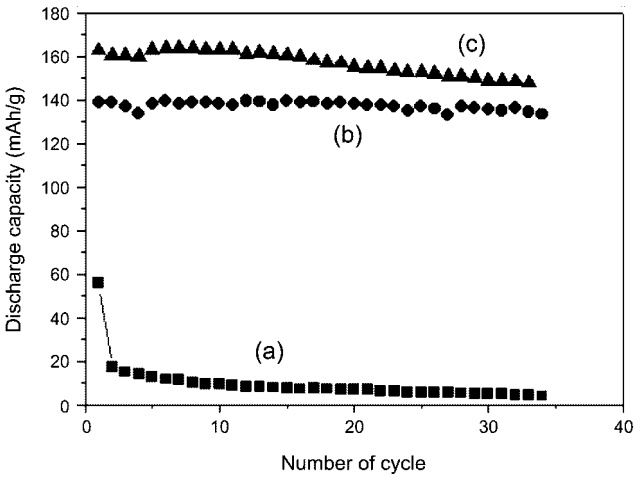

Fig. 3. Plots of specific discharge capacity vs. number of cycles for the Li/$LiPF_6$-EC/DMC (vol 1 : 2)/$LiNiO_2$ powders prepared at various O_2 flow rates at 750 °C. Cycling was carried out galvanostatically at a constant charge/discharge current density of 0.4 mAcm^{-2} between 3.0-4.3 V at room temperature: (a) 300 sccm, (b) 500 sccm, and (c) 800 sccm.

Fig. 3 shows plots of the discharge capacity measured at room temperature versus cycle number for samples prepared at 300, 500, and 800 sccm, respectively. The Li/$LiPF_6$-EC/DMC (1 : 2 by vol.)/$LiNiO_2$ cells were fabricated by using the sample powders synthesized at various O_2 flow rates. [(a): sample C (300 sccm), (b): sample E (500 sccm), and (c): sample H (800 sccm)]. The discharge capacity of the cell increases with increasing oxygen flow rate. For the 300-sccm O_2 flow rate, the capacity is 56 mAh/g at the 1st cycle and dramatically decreases when the cycle goes below 20 mAh/g. However, unlike sample C, the samples E and H initially deliver high discharge capacities of 163 and 139 mAh/g, respectively. But the capacities decrease very slightly when the cycle number goes to 148 and 135 mAh/g after the 35th cycles with capacity retention rates of 90 and 95%, respectively. This electrochemical behavior is very similar to that of the I(003)/I(104) ratio and impurities observed from the XRD spectra as a function of the O_2 flow rate. The inclusion of the cubic rock-salt phase and impurities in the $LiNiO_2$ powders synthesized at low O_2 flow rates deteriorates the electrochemical properties of the cell.

The chemically analyzed composition of the prepared samples

Table 1. Synthetic conditions and structural parameters of $LiNiO_2$ calcined at 750 °C in O_2 flow

$LiNiO_2$ samples	O_2 flow rate (sccm)	Bragg ratio (I_{003}/I_{104})	Lattice constants (hexagonal)		Measured Li contents
			a (Å)	c (Å)	
A	100	0.6466	2.9814	14.2063	0.99
B	200	0.8852	2.8906	14.2134	0.99
C	300	0.9038	2.8902	14.2207	0.99
D	400	1.1773	2.8832	14.2068	1.00
E	500	1.5991	2.8793	14.2000	1.00
F	600	1.5974	2.8753	14.1933	1.00
G	700	1.5699	2.8757	14.1948	0.99
H	800	1.6155	2.8747	14.1892	1.00
I	900	1.5699	2.8779	14.2000	0.99

is listed in Table 1 as a function of oxygen flow rate, together with the calculated composition as well as their XRD data. Chemical analysis shows that the real composition of the lithium element for the synthesized $LiNiO_2$ remains almost 1.0 for all the oxygen flow rates. Although not presented in this paper, SEM photographs show no difference in the average particle size of $LiNiO_2$ powders prepared at all the O_2 flow rates (0.2-0.5 μm).

The structure of $LiNiO_2$ is based on a close-packed network of oxygen anions with the ordering of the Li^+ and Ni^{3+} ions on alternating (111) planes of a cubic rock-salt structure [Delmas and Dresselhaus, 1986]. The pre-calcination of the gel precursors might produce the deposition of carbonaceous residues, originating from the starting materials, which contain CH_3 and COO radicals. In the post calcinating process, higher oxygen flow rates might completely remove this carbonaceous residue in forms of CO_2, CO, and H_2O by reacting with oxygen. But at lower oxygen flow rates the residue easily reacts with lithium to induce the formation of LiOH, Li_2CO_2, and Li_2O impurities in $LiNiO_2$. Moreover, $LiNiO_2$ crystallizes into a cubic rock-salt structure rather than a layered rock-salt structure since 6c sites are insufficiently occupied by oxygen. The layered $LiNiO_2$ is easily contaminated by the cubic rock-salt domain since the structure of layered $LiNiO_2$ is thermodynamically more unstable than that of cubic $LiNiO_2$ [Ohzuku et al., 1993]. This was explicitly evidenced not only by the I(003)/(104) peak ratio, but also from hexagonal lattice parameters a and c shown in Table 1. As the O_2 flow rate increases, the intensity ratio of the (003) and (104) peaks increases up to 500 sccm and remains almost constant when the O_2 flow rate further increases, whereas the parameters a and c decrease with an increasing oxygen flow rate. The increase of a and c with the decrease of the O_2 flow rate reflects the increase in the number of Ni^{2+} rather than Ni^{3+} in the lithium nickel oxide. The Ni^{2+} ions partly enter into the lithium layer, which causes the cation mixing in $LiNiO_2$. The increased degree of cation mixing results in the transformation of the layered to cubic $LiNiO_2$ structures, which may interrupt the motion of the lithium ions leading to the deterioration of the electrode performance during charge and discharge because the cubic structure requires a three-dimensional movement of the Li ions [Kubo et al., 1997].

3. Effect of Sulfur Doping

Oxysulfide layered $LiNiO_{2-y}S_y$ powders (y=0, 0.1, and 0.3) were prepared by using sulfur powders to see the effect of sulfur content doped in the material on the electrode performance. The chemical analyses showed that the actual compositions of the synthesized $LiNiO_2$, $LiNiO_{1.9}S_{0.1}$, and $LiNiO_{1.7}S_{0.3}$ powders are $Li_{0.98}NiO_2$, $Li_{1.01}NiO_{1.98}S_{0.02}$, and $Li_{1.04}NiO_{1.97}S_{0.03}$, respectively.

Fig. 4 shows XRD patterns for the prepared samples. Fig. 4(a) is an XRD pattern for undoped $Li_{0.98}NiO_2$, whereas Fig. 4(b) and (c) are XRD patterns for $Li_{1.01}NiO_{1.98}S_{0.02}$ and $Li_{1.04}NiO_{1.97}S_{0.03}$ powders, respectively. XRD spectra show that all the prepared samples have typical $LiNiO_2$ layered structure with space group $R\bar{3}m$. Any impurity-related peaks are not detectable by the XRD spectra of $Li_{0.98}NiO_2$ and $Li_{1.01}NiO_{1.98}S_{0.02}$ powders [Fig. 4(a) and (b)], whereas the XRD peak of LiOH impurity appears at $2\theta=22^o$ from the $Li_{1.04}NiO_{1.97}S_{0.03}$ powders, although the magnitude of its inclusion is very low. All the peaks that appeared from the XRD patterns were identified with the characteristic peaks of $LiNiO_2$ reported in the X-ray powder data file of JCPDS as well as previously reported works

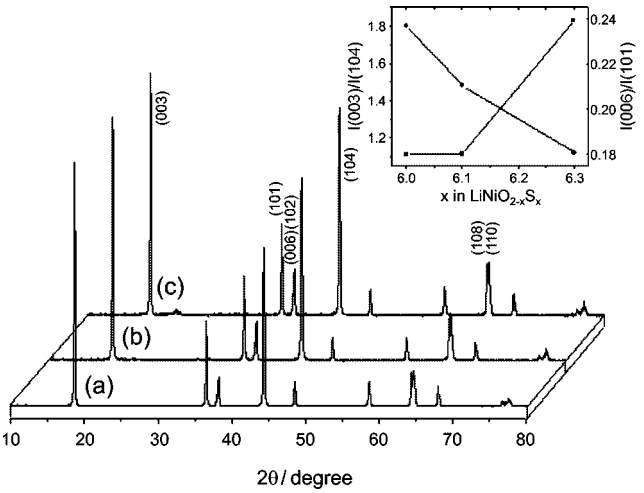

Fig. 4. X-ray diffraction patterns for (a) $Li_{0.98}NiO_2$, (b) $Li_{1.01}NiO_{1.98}S_{0.02}$, and (c) $Li_{1.04}NiO_{1.97}S_{0.03}$ powders prepared by using sulfur powders at a pre-calcination temperature of 450 °C. The gel precursors were calcined at 750 °C in O_2. The upper inset shows the integrated intensity ratios of I(003)/I(104) and I(006)/I(101) peaks as a function of sulfur content.

[Ohzuku et al., 1993].

The lattice constants, a and c, of the synthesized materials were calculated by the Rietveld refinement by using the XRD data of Fig. 4. The lattice constants a and c were identified to remain almost constant at about 2.88 and 14.19 Å, respectively, for all the prepared powders even though the sulfur content in the material was increased. This is because the amount of actually doped sulfur is very low in $LiNiO_{2-y}S_y$, as demonstrated in the chemical analysis. The previous works reported that the lattice constant of a and c of a typical $LiNiO_2$ layered structure are 2.88 and 14.18 Å, respectively [Ohzuku et al., 1993].

The electrochemical properties of $LiNiO_2$ have been estimated by measuring the integrated intensities of (003), (104), (006), and (101) peaks from XRD patterns [Ohzuku et al., 1993; Banov et al., 1995; Morales et al., 1990]. The integrated intensities of (003), (104), (006), and (101) peaks were evaluated from the XRD patterns of Fig. 4 and the integrated intensity ratios of (003)/(104) and (006)/(101) peaks depicted in the upper inset of Fig. 4. With increasing the sulfur content in the material, the intensity ratio of (003)/(104) peaks decreases from 1.5 to 1.12, whereas that of (006)/(101) peaks increases from 0.18 to 0.24. Previous studies report that the $LiNiO_2$ cathode material produces a strong electrochemical property when the intensity ratio of (003) and (104) peaks is higher than 1.2, while that of (006) and (101) peaks is lower than 1.0. Our data show that the initial discharge capacity of our prepared samples will decrease with an increasing sulfur content in the prepared samples.

The morphology of the powders was also observed with an SEM. Fig. 5(a) and (b) show SEM photographs for $Li_{0.98}NiO_2$ and $Li_{1.01}NiO_{1.98}S_{0.02}$ powders, respectively. The shape of $Li_{1.01}NiO_{1.98}S_{0.02}$ powders is a little bit different from that of $Li_{0.98}NiO_2$. The $Li_{0.98}NiO_2$ powders are shaped into a spherical structure, but the $Li_{1.01}NiO_{1.98}S_{0.02}$ powders show a more rectangular shape. The average particle sizes of the powders are about 0.2-0.5 μm for $Li_{0.98}NiO_2$ and 0.5-1 μm for $Li_{1.01}NiO_{1.98}S_{0.02}$ powders, respectively. The rectangular shape of

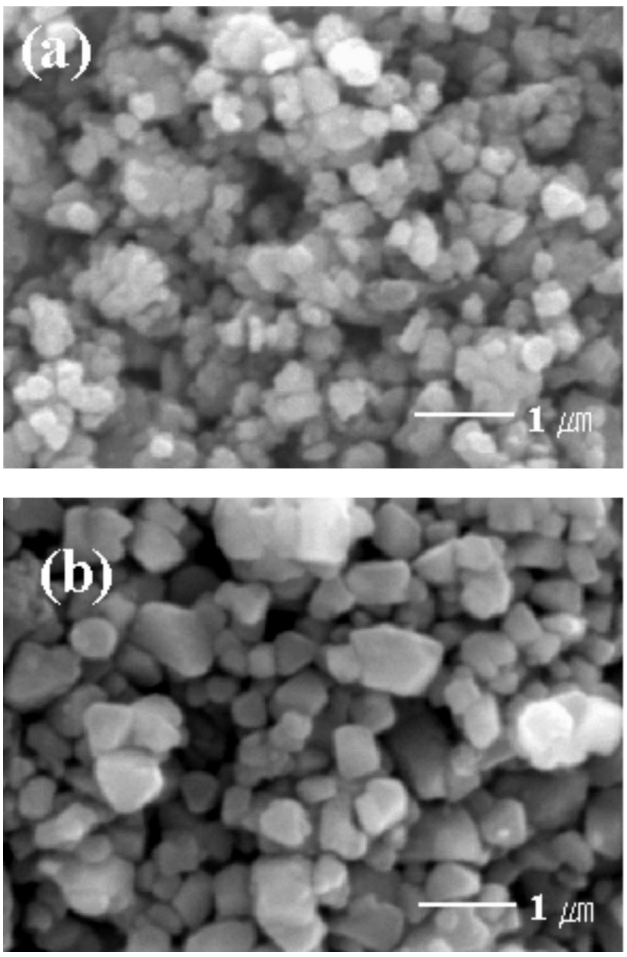

Fig. 5. Scanning electron micrographs for (a) $Li_{0.98}NiO_2$ and (b) $Li_{1.01}NiO_{1.98}S_{0.02}$.

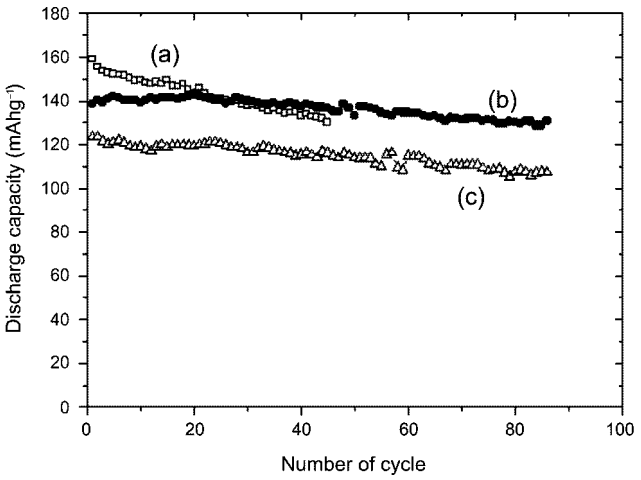

Fig. 6. Plots of specific discharge capacity vs. number of cycles for the Li/$LiPF_6$-EC/DMC(vol 1 : 2)/$LiNiO_{2-y}S_y$ powders. Cycling was carried out galvanostatically at a constant charge/discharge current density of 0.4 mAh/cm^2 between 3.0-4.3 V at room temperature. (a) $Li_{0.98}NiO_2$, (b) $Li_{1.01}NiO_{1.98}S_{0.02}$, and (c) $Li_{1.04}NiO_{1.97}S_{0.03}$.

the powders indicates that the $Li_{1.01}NiO_{1.98}S_{0.02}$ powders have a highly crystallized layered structure. At present, it seems that the structure of $LiNiO_2$ is strongly stabilized by the S-doping. We observed in our previous work that S-doped $LiMn_2O_4$ powders maintain its original structure even after several charge-discharge cycles [Park et al., 2000].

Shown in Fig. 6 are plots of the discharge capacity measured at room temperature versus cycle number for the Li/$LiPF_6$-EC/DMC (1 : 2 by vol.)/$LiNiO_{2-y}S_y$ cells fabricated by using the synthesized sample powders. The cells were tested under a constant charge/discharge current density of 0.4 mA/cm^2 (C/3) between 3.0 and 4.3 V. Fig. 6(a) shows the discharge capacity of the cell fabricated with undoped $Li_{0.98}NiO_2$ powders for comparison. The $Li_{0.98}NiO_2$ cells initially delivered a discharge capacity of 160 mAh/g. But the capacity gradually decreases with the cycle number to be 130 mAh/g after the 45th cycle. For the $Li_{1.01}NiO_{1.98}S_{0.02}$ and $Li_{1.04}NiO_{1.97}S_{0.03}$ cells, meanwhile, the capacity retention rates are significantly improved although the initial capacity of the cells decreases with the increase of the sulfur content doped in $LiNiO_{2-y}S_y$. For example, $Li_{1.01}NiO_{1.98}S_{0.02}$ shows an initial capacity of 140 mAh/g and has the capacity of 130 mAh/g even after the 85th cycle. This corresponds to 93% of its initial capacity. The reduction of the initial capacity by increasing the S content in the $LiNiO_{2-y}S_y$ powders is due to the decrease of the amount of extractable lithium, as anticipated in the Fig. 4 inset. The removal of lithium from the layered nickel oxides is accompanied by an oxidation of Ni^{3+} to Ni^{4+}. In addition, the initial capacity of the $LiNiO_2$ electrode varies depending on the amount of inserted/extracted Li ions. In our experiments, the chemical analysis of the S-doped samples showed that the Li content increases with the increase of the S amount doped in $LiNiO_{2-y}S_y$, resulting in the decrease of the average oxidation state of Ni. For S-doped lithium nickel oxides, therefore, partially substituted S decreases the oxidation state of Ni^{3+} into Ni^{2+}, leading to the reduction of inserted/extracted Li ions because the Ni^{2+} easily forms a stable structure in the lattice. This causes the decrease of the initial capacity as the content of S doped in $LiNiO_{2-y}S_y$ powders increases. However, the retention ratio of the discharge capacity was improved for the sulfur doped oxysulfide $LiNiO_{2-y}S_y$. In the S-doped layered NiO_2 framework, it is assumed that the partial substitution of oxygen with sulfur for $LiNiO_2$ might create a more flexible structure because the electronegativity of sulfur is lower than that of oxygen, which prevents the disintegration of the structure by the elongation between layers caused by the intercalation/deintercalation of lithium ions during the charge-discharge cycles. It also seems that this behavior is attributed to the increases in the Li^+ ion transport by the sulfur doping. According to the electrochemical study on thiospinel ($Li_xTi_2S_4$) structure [Goodenough, 1994], the relatively large size and polarizability of sulfur ions makes it easy for lithium ions to be transported in the oxide structure, which reduces the structural strains of the material formed in the process of Li ion insertion. Another possible cause might be the catalytic activity of the sulfur element in the synthetic process of the S-doped Ni phase. Some previous studies examined the catalytic activity of sulfur in oxidation process of metals [Fatcasiu and Li, 1997]. Fig. 5 shows that the particle size of $Li_{1.01}NiO_{1.98}S_{0.02}$ powders are larger than that of $Li_{0.98}NiO_2$. This suggests that sulfur might act as a catalyst in the synthetic process of S-doped $LiNiO_2$ and thus increase the particle size and enhance structural stability. At this moment, consequently, we speculate that the substitution of a small

amount of S for O not only stabilizes the structural integrity of the electrode material, but also increases the Li^+ ion transport in the electrode which in turn increases electrode performance.

CONCLUSIONS

It was found that oxygen plays an important role for the synthesis of highly crystallized $LiNiO_2$. The deficiency of oxygen during the crystallization process of $LiNiO_2$ induces the formation of impurities in $LiNiO_2$ and contaminates $LiNiO_2$ with a cubic rock-salt domain. The deterioration of the $LiNiO_2$ crystallinity results in the decrease of discharge capacity and poor cycleability. The $Li_{0.98}NiO_2$ cells initially deliver a discharge capacity of 160 mAh/g. But this capacity gradually decreases with the cycle number. For $Li_{1.01}NiO_{1.98}S_{0.02}$, and $Li_{1.04}NiO_{1.97}S_{0.03}$ cells, the capacity retention rates are significantly improved. But the initial capacity of the cells decreases with the increase of sulfur content doped in the material.

ACKNOWLEDGEMENTS

This work was supported by Korea Research Foundation Grant (KRF-2000-E00079).

REFERENCES

Arai, H., Okada, S., Sakurai, Y. and Yamaki, J., "Electrochemical and Thermal Behavior of $LiNi_{1-z}M_zO_2$ (M=Co, Mn, Ti)," *J. Electrochem. Soc.*, **144**, 3117 (1997).

Banov, B., Bourilkov, J. and Mladenov, M., "Cobalt Stabilized Layered Lithium-nickel Oxides, Cathodes in Lithium Rechargeable Cells," *J. Power Sources*, **54**, 268 (1995).

Choi, Y. M., Pyun, S. I., Bae, J. S. and Moon, S. I., "Effects of Lithium Content on the Electrochemical Lithium Intercalation Reaction into $LiNiO_2$ and $LiCoO_2$ Electrodes," *Journal of Power Sources*, **56**, 25 (1995).

Dahn, J. R., von Sacken, U. and Michel, C. A., "Structure and Electrochemistry of $Li_{1+y}NiO_2$ and a New Li_2NiO_2 Phase with the $Ni(OH)_2$ Structure," *Solid State Ionics*, **44**, 87 (1990).

Delmas, C. and Dresselhaus, M. S., "Alkali Metal Intercalation-deintercalation Reaction in 2D Oxides," (eds.), Intercalation in Layered Materials, NATO. ASI. B, **148**, 155 (1986).

Delmas, C., "Alkali Metal Intercalation in Layered Oxides," *Mater. Sci. Eng.*, **B3**, 97 (1989).

Fatcasiu, D., Li, J. Q. and Cameron, S., "Preparation of Sulfated Zirconia Catalysts with Improved Control of Sulfur Content II. Effect of Sulfur Content on Physical Properties and Catalytic Activity," *Applied Catalysis*, **154**, 173 (1997).

Gao, Y., Yakovleva, M. V. and Ebner, W. B., "Novel $LiNi_{1-x}Ti_{x/2}Mg_{x/2}O_2$ Compounds as Cathode Materials for Safer Lithium-Ion Batteries," *Electrochem. Solid-state Lett*, **1**, 117 (1998).

Goodenough, J. B., "Design Considerations," *Solid State Ionics*, **69**, 184 (1994).

Kubo, K., Fujiwara, M., Yamada, S. and Arai, S., "Synthesis and Electrochemical Properties for $LiNiO_2$ Substituted by Other Elements," *J. Power Sources*, **68**, 553 (1997).

Lee, Y. S., Sun, Y. K. and Nahm, K. S., "Synthesis and Characterization of $LiNiO_2$ Cathode Material Prepared by an Adipic Acid-assisted Sol-Gel Method for Lithium Secondary Batteries," *Solid State Ionics*, **118**, 159 (1999).

Morales, J., Peres-Vicente, C. and Tirado, J. L., "Cation Distribution and Chemical Deintercalation $Li_{1-x}Ni_{1+x}O_2$," *Mat. Res. Bull.*, **25**, 623 (1990).

Nishida, Y., Nakane, K. and Satoh, T., "Synthesis and Properties of Gallium-doped $LiNiO_2$ as the Cathode Material for Lithium Secondary Batteries," *J. Power Sources*, **68**, 561 (1997).

Nitta, Y., Okamura, K., Haraguchi, K., Kobayashi, S. and Ohta, A., "Crystal Structure Study of $LiNi_{1-x}Mn_xO_2$," *J. Power Sources*, **54**, 511 (1995).

Ohzuku, T., Ueda, A. and Nagayama, M., "Electrochemistry and Structural Chemistry of $LiNiO_2$ ($R\bar{3}m$) for 4 Volt Secondary Lithium Cells," *J. Electrochem. Soc.*, **140**, 1862 (1993).

Ohzuku, T., Ueda, A., Nagayama, M., Iwakoshi, Y. and Komori, H., "Comparative Study of $LiCoO_2$, $LiNi_{1/2}Co_{1/2}O_2$ and $LiNiO_2$ for 4 Volt Secondary Lithium Cells," *Electrochimica Acta*, **38**, 1159 (1993).

Ohzuku, T., Yanagawa, T., Kouguchi, M. and Ueda, A., "Innovative Insertion Materials of $LiAl_{1/4}Ni_{3/4}O_2$ ($R\bar{3}m$) for Lithium-ion (shuttlecock) Batteries," *J. Power Sources*, **68**, 131 (1997).

Park, S. H., Park, K. S., Sun, Y. K. and Nahm, K. S., "Synthesis and Characterization of a New Spinel, $Li_{1.02}Al_{0.25}Mn_{1.75}O_{3.97}S_{0.03}$, Operating at Potentials Between 4.3 and 2.4 V," *J. Electrochem. Soc.*, **147**, 2116 (2000).

Reimers, J. N., Li, W., Rossen, E. and Dahn, J. R., "Structure, Diffraction and Energetic Stability of the Spinel Form of $LiCoO_2$," in: MRS Symp. Proc., **293**, 3 (1993).

Wang, G. X., Zhong, S., Bradhurst, D. H., Dou, S. X. and Liu, H. K., "Synthesis and Characterization of $LiNiO_2$ Compounds as Cathodes for Rechargeable Lithium Batteries," *J. Power Sources*, **76**, 141 (1998).